Science of the Total Environment 881 (2023) 163378

Contents lists available at ScienceDirect

Science of the Total Environment

journal homepage: www.elsevier.com/locate/scitotenv

Using in situ measurements of optical brighteners for rapid reconnaissance of wastewater inputs to water resources

Carly R. Finegan *, Elizabeth A. Hasenmueller

Department of Earth and Atmospheric Sciences, Saint Louis University, Saint Louis, MO 63108, United States
WATER Institute, Saint Louis University, Saint Louis, MO 63103, United States

HIGHLIGHTS

- Water managers must identify wastewater inputs to the environment for remediation.
- Traditional wastewater tracers (*E. coli*, F^-) are costly, slow, or complex to measure.
- Optical brightener fluorescence is an inexpensive and easy to use wastewater tracer.
- It is better for identifying wastewater in the environment than traditional tracers.
- Water managers can use optical brightener fluorescence as a reconnaissance tool.

GRAPHICAL ABSTRACT

Field optical brightener fluorescence readings are the most effective way to rapidly detect wastewater inputs to water resources.

Method	Optical brighteners	*E. coli*	MST	B	F^-
Simple?	✓	✓	✗	✗	✗
Inexpensive?	$	$	$$$	$$	$$
Unique to source?	✓	✗	✓	✗	✗
In situ reading?	✓	✗	✗	✗	✗

ARTICLE INFO

Editor: Jay Gan

Keywords:
Water quality
Urban geochemistry
Sewage contamination
Water sourcing
Environmental tracers

ABSTRACT

Untreated wastewater entering the environment through leaking infrastructure and sewer overflows threatens both human and aquatic health. Water managers therefore need low cost, in situ methods to detect sewage contamination in real time to promptly employ mitigation strategies. However, wastewater has traditionally been identified in waterbodies using chemical and microbial tracers and indicators that can be non-unique to wastewater and often require complex and expensive analyses. Optical brighteners (synthetic brightening compounds present in laundry detergents and paper products) are emerging as ideal tracers of wastewater because of their quick and inexpensive field detection using handheld fluorometers. To test the efficacy of optical brighteners as standalone, in situ wastewater tracers, field readings of their fluorescence were compared with traditional wastewater analytes (e.g., B, F^-, microbial indicators) at multiple points in time and space for a suburban watershed (Fishpot Creek, Saint Louis, Missouri, United States). We also used chemical tracers in three mixing models of endmembers to assess the wastewater fraction across the watershed. Compared to other analytes, optical brightener fluorescence measurements had the strongest correlation with wastewater infrastructure density ($r = 0.71$, $p < 0.05$), indicating their utility as tracers. All our endmember mixing models employing optical brightener readings predicted positive and significant correlations between the untreated wastewater fraction in streamflow and sewer pipe density at each site ($r \geq 0.77$, $p < 0.05$). While using optical brightener readings for wastewater detection has some limitations (e.g., minor photodegradation), we found them to be more robust tracers than other analytes. Thus, optical brightener fluorescence measurements are an ideal initial screening tool for identifying wastewater contributions to the environment.

1. Introduction

Waterbodies contaminated with untreated wastewater threaten human and aquatic health due to the presence of pathogens, excess nutrients, pharmaceutical compounds, and heavy metals. Thus, water management

* Corresponding author at: Department of Earth and Atmospheric Sciences, Saint Louis University, Saint Louis, MO 63108, United States.
E-mail address: carly.finegan@slu.edu (C.R. Finegan).

http://dx.doi.org/10.1016/j.scitotenv.2023.163378
Received 2 December 2022; Received in revised form 30 March 2023; Accepted 4 April 2023
Available online 11 April 2023

authorities are particularly concerned with identifying locations where untreated wastewater enters the environment so that they can remediate infrastructure issues that jeopardize water resources and aquatic ecosystems. While point sources of untreated wastewater are readily identifiable in watersheds (e.g., sewer overflows), detecting sewage exfiltration from leaking septic systems or sewer mains and laterals presents a considerable challenge to water managers.

To locate untreated wastewater inputs to waterbodies, chemical and biological tracer and indicator studies are often employed. "Ideal" wastewater tracers are conservative (non-reactive), either unique to wastewater or present in markedly different amounts in wastewater versus other water sources, at concentrations above instrument detection limits, and at consistent concentrations in the endmembers over time (Rabiet et al., 2005; Dickenson et al., 2011; Van Stempvoort et al., 2013). However, water managers also benefit from tracers that are quick, easy, and inexpensive to measure on site so that they can rapidly evaluate potential sources of untreated wastewater to areas of concern.

Traditional wastewater tracers and indicators often present multiple challenges for water managers, including confounded signatures due to sources other than wastewater, the need for highly technical equipment, expensive analyses, or the lack of real-time data. For instance, fecal indicator bacteria, like *Escherichia coli* (*E. coli*), are relatively inexpensive to measure, easy to quantify, and recommended by the United States Environmental Protection Agency (USEPA) to detect fecal contamination of recreational waters (USEPA, 2018). However, high levels of *E. coli* in water resources can be the result of inputs from agricultural runoff, urban runoff, pet and wildlife waste, or untreated sewage (Anderson et al., 2005; Dickerson et al., 2007), convoluting attempts to identify the wastewater signature in many settings. Fecal contamination sources can be distinguished with microbial source tracking (MST; Dickerson et al., 2007; Bird et al., 2019; Devane et al., 2019), but these analyses are too laborious, technical, expensive, and slow for many applications. Inorganic species like F^-, from fluoridated drinking water that enters wastewater systems (Meenakshi and Maheshwari, 2006), and total B, from B-containing bleaching agents in cleaning products introduced during water use (Vengosh et al., 1994; Petelet-Giraud et al., 2009; Hasenmueller and Criss, 2013; Lockmiller et al., 2019), are normally elevated in wastewater compared with most natural waters, but they cannot be detected in the field, limiting real-time assessments of wastewater inputs.

Optical brighteners may be ideal tracers for identifying wastewater inputs to the environment because they are unique to anthropogenic sources, with few common origins other than sewage. They are a group of synthetic fluorescent compounds that absorb near-ultraviolet light (360–365 nm) and fluoresce blue light (415–445 nm; Tavares et al., 2008). Because of these properties, 90 % of optical brighteners in the United States are used in laundry detergents to whiten and brighten clothing, with other uses including whitening paper products like toilet paper (Hagedorn et al., 2005a). When clothing is washed, 25–95 % of the optical brighteners in the detergent bind to the clothes and the remainder is transported with wastewater to sewage or septic systems (Poiger et al., 1998). The breakdown of toilet paper after use adds additional optical brighteners to wastewater (Hagedorn et al., 2005b). High concentrations of optical brighteners thus occur in influent wastewater, making them a suitable tracer of untreated sewage (Poiger et al., 1998).

Preliminary applications of optical brighteners to test wastewater inputs to the environment have relied on comparison with only a few other tracers (e.g., *E. coli*) or analyses with complex and costly laboratory equipment (Hartel et al., 2007; Tavares et al., 2008; Cao et al., 2009; Dubber and Gill, 2017). Laboratory studies comparing optical brightener fluorescence measurements using both inexpensive field equipment and training-intensive and expensive laboratory instrumentation have shown the methods to be equally effective (Hartel et al., 2007; Cao et al., 2009). However, to our knowledge, no one has tested the application of handheld fluorometers as a standalone technique for in situ detection of optical brighteners in waterbodies.

Our study therefore investigates if field fluorescence measurements for optical brighteners with an inexpensive, handheld fluorometer can be used as in situ tests to detect non-point sources of untreated wastewater inputs to the environment. Rapid and inexpensive field assessments for wastewater releases is an urgent need for water managers to proactively remediate infrastructure problems. We compare high resolution spatial and temporal field fluorescence data for optical brighteners with their laboratory fluorescence readings, traditional wastewater tracers and indicators (e.g., B, F^-, *E. coli*, MST), and the apportioned wastewater contributions estimated from endmember mixing analyses for a suburban watershed that features an aging wastewater infrastructure system.

2. Study site

We tested the use of optical brighteners for detection of wastewater exfiltration from municipal infrastructure (e.g., leaks from main and lateral sewer lines) and septic systems in the Fishpot Creek watershed, which is located near Saint Louis, Missouri, (Fig. 1a) in the suburb of Valley Park, Missouri. The basin is 28.2 km^2, has 30.4 % impervious surface area (ISA), and is in a suburban-residential area. Watershed ISA (Fig. 1b) is the highest in the northern portion of the basin, where high intensity developed areas along a busy road (Missouri Route 100) intersect the stream. The southern portion of the catchment features lower ISA and development, having parks with wooded wetlands, pastures, and mixed forests. A stream reach near the outlet of the basin that is classified for use (whole body contact category B; WBC-B) has been included on the Missouri Department of Natural Resources' (MoDNR) 303(d) list of impaired waters for *E. coli* geometric means exceeding the recreational season (April 1 to October 31 in a given year; Missouri Department of Natural Resources MoDNR, 2016a) regulatory limit of 206 colony-forming units (CFU) per 100 mL (Missouri Department of Natural Resources MoDNR, 2016). Fishpot Creek is an ideal study site for testing the use of optical brighteners as a rapid reconnaissance tool to locate wastewater inputs because of its history of *E. coli* contamination and the need to update wastewater infrastructure in the watershed (see Supplemental Material Section 1.1 for additional detail).

The Fishpot Creek catchment features differing drainage attributes based on its geology (see Supplemental Material Section 1.2 for information on watershed geology) and topography, so we hereafter describe segments of the basin as the: "east branch", "west branch", and "outlet" (Fig. 1c). The east and west branches are separate drainage subbasins that combine in the south section of the watershed to form the outlet. The southern portions of the east and west branches are ephemeral, often resulting in no surface water flowing through these reaches during dry weather. The outlet is fed by karst springs, including Pettys Spring (Site 0) and nearby Bright Spring (Missouri Department of Natural Resources MoDNR, 2016a). Fishpot Creek drains into the Meramec River, which is a direct tributary to the Mississippi River.

The watershed has separate sanitary and stormwater sewer lines, with raw sanitary sewage conveyed to the Metropolitan Saint Louis Sewer District's (MSD) Grand Glaize Wastewater Treatment Plant for treatment, while stormwater is drained directly into the stream. The plant's processed effluent is released into another catchment (i.e., Grand Glaize Creek), so Fishpot Creek does not feature any discharge sites for treated wastewater effluent. Thus, the only potential wastewater sources to the watershed are exfiltration from municipal sanitary sewers (e.g., leaks from main or lateral sewer lines) or septic systems and discharges from stormwater sewer lines.

Drinking water distributed to homes and businesses in the Fishpot Creek basin is known to enter the stream (Lockmiller et al., 2019), which is potentially due to infrastructure leaks or lawn irrigation practices. The drinking water is sourced from the Missouri River and fluoridated during treatment to 700 μg/L F^- (USDHHS, 2015; Missouri American Water, 2019). This F^- concentration is an order of magnitude higher than the natural background level of F^- for regional streams that have limited

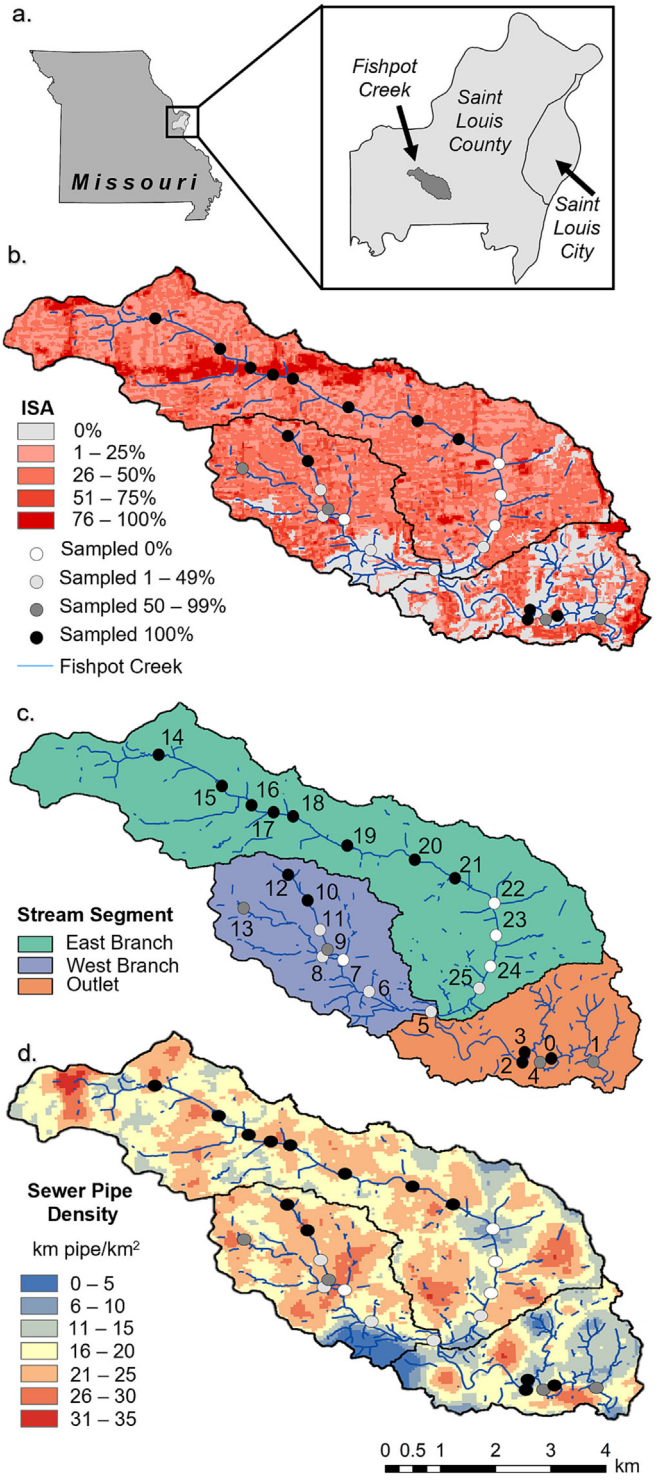

Fig. 1. The Fishpot Creek watershed with (a) its location in relation to the state of Missouri, Saint Louis County, and the City of Saint Louis, (b) ISA (data from Homer et al., 2015), (c) delineated subbasins with sampling locations and their identification codes, and (d) sewer pipe density (data from MSD, 2019).

municipal water inputs (~75 μg/L; Lockmiller et al., 2019). The Missouri River source water also features naturally higher concentrations of some major (e.g., Na^+, SO_4^{2-}) and minor (e.g., total B) ions and elements compared to local water types (Criss et al., 2001; Hasenmueller and Criss, 2013). The local drinking water is therefore chemically unique from the stream water.

3. Methods

3.1. Field procedures

In situ measurements and samples from the Fishpot Creek basin were collected at high spatial and temporal resolution to assess variations in optical brightener levels and their relationship to other chemical and biological tracers and indicators of wastewater. We sampled 26 sites in the watershed (Sites 0–25; Fig. 1), including sites on the mainstem of Fishpot Creek, tributary streams, and groundwater inflow (i.e., Pettys Spring; Site 0), monthly from June 2019 through October 2020. Sites were chosen to maximize coverage across the watershed, the range in nearby sewer infrastructure density (see Supplemental Material Section 2.1 for methodology to determine infrastructure density), and accessibility. To avoid the confounding effects of recent precipitation, which could result in stormwater inflow to the stream, monthly site visits occurred during "baseflow" conditions. We define baseflow as streamflow at least 3 days following a precipitation event that is near the seasonal average for discharge. To understand any rapid changes in analyte values in the stream water, weekly sample collection and continuous water quality monitoring occurred near the basin outlet (Site 2; Fig. 1), where a United States Geological Survey (USGS) stage and discharge gauging station is located (gauge number 07019120; USGS, 2022).

3.1.1. In situ measurements

For both the monthly and weekly watershed sampling events, we measured in situ water quality parameters using a Turner Designs AquaFluor Handheld Fluorometer (optical brightener fluorescence), a YSI Professional Plus Multiparameter Instrument (temperature, specific conductivity, pH, dissolved O_2, Cl^-), and a Hach 2100P Portable Turbidimeter (turbidity). We also tested the variability of optical brightener fluorescence readings over short periods in the field during site visits. To do so, readings were made 3–4 times within a 15-min period for a subset of the monthly (August 2020 through September 2020) and weekly (August 2020 through October 2020) sampling events. A YSI EXO2 Multiparameter Sonde collected in situ water quality measurements at the weekly sampling site (Site 2), including temperature, specific conductivity, pH, Cl^-, turbidity, and fluorescing dissolved organic matter (fDOM), every 5 min.

3.1.2. Sample collection and preservation

Optical brightener photodecay test samples were collected for a subset of the monthly sampling events (January 2020 to February 2020 and June 2020 to October 2020) using 500-mL opaque low-density polyethylene bottles. During all sampling events, water samples for ion and elemental analyses were field-filtered through 0.2-μm cellulose acetate membrane filters. Subsamples for anion chemistry via ion chromatography (IC) received no further treatment, while subsamples for metal and metalloid chemistry via inductively coupled plasma optical emission spectrometry (ICP-OES) were acidified to 1 % with HNO_3. Total organic C (TOC), as non-purgeable organic C (NPOC), samples were collected only for the October 2020 monthly sampling event. Water samples for *E. coli* enumeration were collected for monthly spatial samplings during part of the recreational season of 2019 (June 2019 to October 2019) and during the complete recreational season of 2020 (April 2020 to October 2020). The samples for *E. coli* testing were placed in autoclaved 500-mL polypropylene bottles. Water samples for MST were collected during the October 2020 monthly sampling event in the same manner as the *E. coli* samples. The optical brightener photodecay, ICP-OES, and *E. coli* samples were stored at 4 °C until analysis, while IC, TOC, and MST samples were frozen until analysis.

We also collected samples to characterize three potential endmember contributions to Fishpot Creek's flow: "natural water", wastewater, and drinking water. The "natural water" endmember represents baseflow supplied to the stream without contributions from municipal water sources. Because of high development throughout the basin, none of our sites were suitable to serve as the natural endmember. We instead used groundwater samples from a nearby (13 km west) rural karst spring (Rockwoods Spring;

Wildwood, Missouri) with 3 % catchment-wide ISA (Robinson and Hasenmueller, 2017) to characterize the natural endmember. Samples from Rockwoods Spring were collected within a week of the monthly sampling events. Within 2 days of the monthly sampling suites, 24-h composite influent, untreated wastewater samples were obtained from the MSD Grand Glaize Wastewater Treatment Plant to determine the chemistry of any potential contributions from the municipal wastewater endmember. Only influent wastewater samples were considered in our study because the watershed does not have any treated effluent discharge sites and our baseflow sampling regime was designed to preclude stormwater contributions. Treated drinking water samples were collected from businesses within the Fishpot Creek watershed in June 2021 and July 2021 to characterize the drinking water endmember, which can enter the stream through infrastructure leaks or irrigation.

3.2. Laboratory measurements

3.2.1. Optical brighteners

All our presented optical brightener values are the raw, uncorrected fluorescence measurements reported in reference fluorescence units (RFU). We did not correct our field optical brightener readings for temperature, turbidity, or organic matter content in the laboratory because we wanted to understand the utility of using in situ optical brightener readings as a standalone reconnaissance tool without introducing additional (and potentially expensive, time consuming, or laborious) analyses. Following the methods of Cao et al. (2009) and Dubber and Gill (2017), photodecay tests were conducted in the laboratory immediately upon our return from the field in an attempt to distinguish optical brightener and organic matter fluorescence signals in the water samples. These studies found that optical brighteners and organic matter can fluoresce at similar wavelengths but differ in their photodecay patterns when exposed to an ultraviolet light source. The specific details of the photodecay testing methodology are outlined in Supplemental Material Section 2.2.

3.2.2. Other chemical species

Anion (F^-, Cl^-, SO_4^{2-}) concentrations were measured using a Thermo Scientific Integrion Dionex HPIC IC. Total metal and metalloid (B, Ca, Mg, Sr, K, Na) concentrations were measured using a PerkinElmer Optima 8300 ICP-OES. Check standards, replicate samples, and blanks were included with all runs to assess instrument accuracy and precision. Both accuracy and precision were within 5 % for the IC, while accuracy was within 10 % and precision was within 5 % for the ICP-OES. Samples collected in October 2020 for TOC were sent frozen to the National Great Rivers Research and Education Center (NGRREC) for analysis on an Elementar vario TOC cube (as NPOC). Accuracy and precision were within 8 % and 1 %, respectively.

3.2.3. Bacteria

Total coliform and *E. coli* most probable numbers (MPN) were analyzed in the laboratory immediately following sample collection using the USEPA-approved IDEXX Colilert and Quanti-Tray 2000 system (IDEXX Laboratories, 2013, 2017). The measurement range is from <1.0 to >2,419.6 CFU/100 mL, with concentrations derived from the method's MPN table. While coliform bacteria are indicative of fecal contamination, they can have multiple sources, making these bacteria a non-unique tracer. To constrain human-derived fecal contamination in the Fishpot Creek watershed, water samples collected during the October 2020 sampling event (i.e., on October 26, 2020) underwent MST analysis of the HF183 marker in the fecal-associated bacteria, *Bacteroides*, using quantitative polymerase chain reaction (qPCR) assay. We filtered 100 mL of sample from each site within 6 h of collection using a 0.4-μm cellulose acetate membrane filtration funnel assembly. Filters were folded, placed in extraction tubes containing glass beads, stored at −80 °C, then shipped overnight on dry ice to the Northeastern Ohio Regional Sewer District (NEORSD) for DNA extraction and purification using a modified version of USEPA Method 1696 (USEPA, 2019; see Supplemental Material Section 2.3 for more detail).

3.3. Endmember mixing analyses

The percent contribution of wastewater to the total flow for each site in the Fishpot Creek catchment was calculated using three models of endmember mixing. A simple, two component mixing model, using field optical brightener fluorescence values as the only chemical tracer (C), was used to determine the wastewater fraction for stream and spring water samples. The mixing model, modified from Sklash et al. (1976), determines an endmember's fraction (α) of the total flow using the equation:

$$C_S = \alpha_N C_N + \alpha_W C_W \quad (1)$$

The subscripts represent the sample (S), natural water endmember (N), and wastewater endmember (W). The natural water endmember signifies unimpacted baseflow to the catchment and was characterized by the Rockwoods Spring samples. The wastewater endmember data for this calculation were the 24-h composite untreated influent wastewater samples from MSD's Grand Glaize Wastewater Treatment Plant. We did not consider treated wastewater because effluent discharge sites are not present in the Fishpot Creek basin, have locations known to water managers, and do not present the same environmental risks as untreated wastewater. Inputs from the stormwater sewers were not expected during baseflow conditions, so we did not characterize this water type. The two component mixing model approach was tested as a simple endmember separation method for water managers to quickly assess untreated wastewater inputs to a site using only in situ optical brightener data.

We also employed three component and inverse mixing models that included natural water and wastewater contributions, like the two component mixing model, but accounted for potential inputs of a second municipal water type: a drinking water endmember (D), which is known to enter Fishpot Creek (Lockmiller et al., 2019) likely due to leaking infrastructure or lawn irrigation practices. For both models, the endmember signatures in the stream or spring water samples are expressed as:

$$C_S = \alpha_N C_N + \alpha_W C_W + \alpha_D C_D \quad (2)$$

While wastewater originates, in part, from drinking water, the drinking water endmember is geochemically distinct from the influent wastewater endmember because of additions during water use (e.g., inputs of optical brighteners and B from detergents). The three component and inverse mixing models included more analytes than the two component mixing model and are therefore generally considered more robust analyses of endmember inputs.

Our three component mixing model, after Lee and Krothe (2001), used two tracers to determine endmember proportions for each model run. We used three combinations of tracer data in the model: optical brighteners and B, optical brighteners and F^-, and B and F^-. These tracers were chosen because they have few non-municipal water sources, differ substantially among the endmembers, and are generally considered to be conservative (Kennedy et al., 1991; Cao et al., 2009; Dubber and Gill, 2017; Guinoiseau et al., 2018; Lockmiller et al., 2019).

For the inverse mixing model, we used optical brightener, B, F^-, Ca, Mg, Sr, and K values (i.e., a total of seven tracers used simultaneously in the model) to determine natural water, wastewater, and drinking water contributions to flow. Other studies that have used inverse mixing models have included additional analytes, like Na^+, Cl^-, and SO_4^{2-} (Négrel et al., 1993; Roy et al., 1999). We did not include these analytes in our inverse mixing model because other sources for these tracers (e.g., basin-wide winter road deicing applications of Na^+ and Cl^- and atmospheric and fertilizer inputs of SO_4^{2-}) confound the results. Following the work of Lockmiller et al. (2019) and references therein, a least squares method was used to solve for the proportions of different endmembers for the inverse mixing model because the system is over-constrained. For both the three component and inverse mixing models, 10,000 random endmember composition combinations were sampled from uniform distributions of endmember values to account for the uncertainty and high variability in

Table 1
Averages and standard deviations for analytes at each Fishpot Creek sampling site for the monthly watershed samples (Sites 0–25), weekly samples at Site 2, and monthly endmember samples.

Sample	*n*	OB (RFU)[a]	B (μg/L)	F^- (μg/L)	Ca (mg/L)	Mg (mg/L)	Sr (μg/L)	K (mg/L)	Na (mg/L)	Cl^- (mg/L)	SO_4^{2-} (mg/L)	Temperature (°C)	Turbidity (NTU)
Site 0 (Pettys Spring)	11	8.3 ± 1.0	41 ± 21	119 ± 27	89.1 ± 16.4	17.0 ± 4.2	250 ± 64	3.5 ± 0.6	85.2 ± 17.2	156.4 ± 31.2	60.4 ± 23.5	14.5 ± 1.1	4.8 ± 2.9
Site 1	17	8.5 ± 1.3	40 ± 14	118 ± 32	90.4 ± 13.7	16.7 ± 3.6	243 ± 45	3.6 ± 0.4	78.5 ± 18.1	135.9 ± 38.0	55.3 ± 20.7	14.5 ± 3.0	8.6 ± 19.1
Site 2	18	10.3 ± 1.7	40 ± 10	83 ± 20	76.4 ± 11.0	12.2 ± 1.9	247 ± 42	4.0 ± 0.7	54.8 ± 19.8	93.0 ± 32.9	40.8 ± 17.2	15.2 ± 7.1	1.4 ± 0.7
Site 3	18	10.7 ± 2.7	38 ± 12	81 ± 19	66.3 ± 12.0	10.7 ± 2.2	227 ± 51	4.0 ± 0.8	52.4 ± 21.6	88.5 ± 34.1	34.8 ± 11.2	16.4 ± 6.7	2.7 ± 3.5
Site 4	16	10.6 ± 1.7	31 ± 7	81 ± 20	67.9 ± 6.6	10.7 ± 1.2	196 ± 22	3.6 ± 0.5	52.8 ± 21.2	85.0 ± 40.8	32.1 ± 6.8	14.7 ± 7.1	2.5 ± 1.6
Site 5	4	12.5 ± 1.6	38 ± 7	73 ± 24	57.0 ± 5.6	8.8 ± 0.9	168 ± 10	3.8 ± 0.7	41.9 ± 28.8	50.6 ± 37.0	22.7 ± 5.3	12.4 ± 11.4	4.4 ± 5.3
Site 6	3	14.8 ± 1.2	10 ± 0	112 ± 10	27.8 ± 6.0	4.9 ± 0.9	99 ± 11	3.0 ± 0.4	29.3 ± 24.2	41.2 ± 41.7	12.5 ± 3.6	15.7 ± 12.2	13.1 ± 7.8
Site 7	0	N/A	N/A	N/A	N/A	N/A	N/A	N/A	N/A	N/A	N/A	N/A	N/A
Site 8	2	18.0 ± 0.9	8 ± 0	95 ± 43	27.1 ± 2.7	4.3 ± 0.9	83 ± 8	3.2 ± 0.5	115.3 ± 4.2	155.3 ± 2.4	16.5 ± 0.9	2.3 ± 0.8	5.8 ± 4.1
Site 9	17	22.1 ± 5.5	28 ± 7	113 ± 32	52.3 ± 12.2	11.2 ± 2.7	163 ± 39	4.5 ± 1.3	69.3 ± 57.2	94.2 ± 86.5	38.0 ± 29.0	13.6 ± 7.2	4.4 ± 7.1
Site 10	17	15.9 ± 4.3	43 ± 13	118 ± 41	92.8 ± 15.5	24.9 ± 4.8	256 ± 37	3.8 ± 0.9	101.5 ± 36.3	154.2 ± 53.1	66.2 ± 36.7	13.4 ± 37.4	1.4 ± 0.8
Site 11	4	16.7 ± 2.7	25 ± 7	107 ± 21	64.5 ± 7.1	15.3 ± 2.1	209 ± 37	3.4 ± 0.7	146.1 ± 64.7	205.8 ± 87.1	54.4 ± 7.5	7.9 ± 7.8	1.3 ± 0.3
Site 12	17	15.3 ± 2.4	115 ± 28	257 ± 85	78.6 ± 6.3	23.2 ± 3.1	350 ± 27	3.3 ± 0.8	94.9 ± 61.8	114.9 ± 111.0	98.7 ± 52.2	14.2 ± 5.7	2.1 ± 2.2
Site 13	11	31.3 ± 12.5	26 ± 25	156 ± 44	41.4 ± 10.4	7.1 ± 2.1	141 ± 36	4.7 ± 3.2	64.6 ± 48.4	108.8 ± 97.4	18.0 ± 11.5	12.8 ± 6.5	21.5 ± 17.8
Site 14	18	15.5 ± 3.8	22 ± 8	106 ± 26	60.6 ± 14.9	9.8 ± 2.6	211 ± 52	3.7 ± 0.9	96.5 ± 55.6	149.6 ± 93.1	44.6 ± 8.3	14.4 ± 6.4	1.9 ± 0.9
Site 15	17	16.5 ± 5.9	30 ± 9	143 ± 37	67.9 ± 8.6	14.8 ± 2.4	230 ± 28	4.1 ± 1.4	87.4 ± 39.1	141.4 ± 62.4	58.3 ± 21.2	14.5 ± 7.6	3.0 ± 2.9
Site 16	18	15.4 ± 2.5	32 ± 10	127 ± 29	77.9 ± 11.1	17.6 ± 2.7	246 ± 30	3.7 ± 0.7	107.5 ± 51.1	190.3 ± 92.2	57.9 ± 22.0	15.5 ± 7.9	6.8 ± 4.4
Site 17	18	14.7 ± 2.6	29 ± 9	128 ± 24	82.4 ± 12.8	18.2 ± 3.5	256 ± 36	3.7 ± 0.7	106.2 ± 40.7	196.9 ± 65.5	56.3 ± 18.9	16.0 ± 8.1	1.4 ± 0.6
Site 18	17	14.3 ± 2.3	40 ± 37	127 ± 30	82.7 ± 10.5	19.5 ± 3.2	269 ± 32	3.7 ± 0.7	106.6 ± 41.0	200.3 ± 68.3	60.7 ± 19.6	16.1 ± 8.5	2.6 ± 1.7
Site 19	18	14.1 ± 3.1	29 ± 9	117 ± 31	79.8 ± 10.6	18.3 ± 3.0	254 ± 31	3.5 ± 0.7	99.7 ± 40.1	174.7 ± 59.9	59.0 ± 19.6	15.8 ± 7.8	1.8 ± 0.7
Site 20	17	14.5 ± 3.0	33 ± 11	141 ± 30	78.1 ± 10.6	19.4 ± 3.1	254 ± 32	3.5 ± 0.7	98.8 ± 36.8	170.7 ± 59.9	65.1 ± 19.9	15.2 ± 7.1	1.5 ± 0.7
Site 21	18	15.2 ± 5.6	31 ± 12	125 ± 25	73.4 ± 14.3	17.7 ± 3.4	237 ± 44	3.4 ± 0.7	92.0 ± 36.0	168.5 ± 54.5	60.8 ± 19.9	17.6 ± 8.7	2.4 ± 2.2
Site 22	0	N/A	N/A	N/A	N/A	N/A	N/A	N/A	N/A	N/A	N/A	N/A	N/A
Site 23	0	N/A	N/A	N/A	N/A	N/A	N/A	N/A	N/A	N/A	N/A	N/A	N/A
Site 24	0	N/A	N/A	N/A	N/A	N/A	N/A	N/A	N/A	N/A	N/A	N/A	N/A
Site 25	1	0.61	28	166	31.0	5.2	101	3.5	19.5	22.8	14.3	24.5	13.6
Weekly samples (Site 2)	76	10.9 ± 3.4	41 ± 10	81 ± 22	74.3 ± 19.0	11.8 ± 3.1	241 ± 58	4.1 ± 0.7	61.8 ± 34.5	103.6 ± 61.2	39.6 ± 16.0	15.1 ± 6.9	3.4 ± 9.6
Natural water (Rockwoods Spring)	18	5.6 ± 2.1	35 ± 5	104 ± 13	94.5 ± 7.3	12.4 ± 3.2	133 ± 25	2.0 ± 0.4	30.1 ± 12.1	58.3 ± 25.5	30.5 ± 10.4	13.1 ± 1.3	2.4 ± 1.6
Untreated wastewater (GGWTP)[b]	17	142.7 ± 56.5[c]	177 ± 59	562 ± 139	57.4 ± 11.9	21.5 ± 3.0	249 ± 30	13.0 ± 3.2	91.6 ± 12.9	118.6 ± 27.4	132.2 ± 31.8	N/A	178.9 ± 77.0
Drinking water (taps)[d]	12	13.9 ± 3.6	53 ± 10	627 ± 23	24.0 ± 3.0	8.9 ± 3.2	136 ± 9	5.1 ± 0.1	24.1 ± 6.4	16.1 ± 2.5	74.6 ± 13.4	N/A	0.6 ± 0.3

[a] The reported optical brightener (OB) sensor response values are raw, uncorrected fluorescence values.
[b] Influent wastewater samples were 24-h composites from the Grand Glaize Wastewater Treatment Plant (GGWTP) in Valley Park, Missouri.
[c] An influent wastewater optical brightener measurement outlier (with a value of 1071 RFU, which is 4 × higher than the next highest influent wastewater sample value) was excluded from the dataset due to differences in the measurement methodology at the start of the study.
[d] Treated drinking water samples were collected from drinking water taps throughout the Fishpot Creek basin.

endmember compositions. From those endmember combinations, 10,000 Monte Carlo simulations were calculated and averaged to get final proportions of the different endmembers. We discarded model results when endmember proportions were negative or did not sum to 1.00 ± 0.05.

4. Results

4.1. Infrastructure distribution

The sewer pipe density for the Fishpot Creek basin was calculated and mapped to help characterize possible untreated wastewater inputs to the sample sites (Fig. 1d; data from MSD, 2019). We defined "sewer pipe density" as the combination of both the sanitary and stormwater infrastructure draining to a given site. We chose to include the stormwater sewers in our calculations because we sampled the catchment at baseflow, eliminating the potential for direct stormwater runoff to the stream. However, the stormwater infrastructure can still convey municipal waters to the stream during low flow conditions due to contributions from sanitary sewer exfiltration, drinking water infrastructure exfiltration, or lawn irrigation practices. We found that sewer pipe density was lowest in the outlet and highest in the west branch (Fig. 1d). We were unable to map treated drinking water infrastructure in the catchment because pipe location data were unavailable for security reasons.

4.2. Endmember characterization

We characterized the natural water, untreated wastewater, and drinking water endmembers (Table 1) that could potentially contribute to flow in the Fishpot Creek watershed. Of the three endmembers, the untreated wastewater had the highest average optical brightener fluorescence value and B concentration, while the drinking water had the highest average F^- concentration (Table 1). The average F^- concentration in the wastewater endmember was ~10 % lower than the drinking water endmember but was within 1 % of wastewater F^- data collected for another study in the region (Lockmiller et al., 2019). Natural water had the lowest values for these analytes of all the endmembers. While we only discuss optical brighteners and the traditional wastewater tracers B and F^- here, additional endmember geochemical data used in our inverse mixing model are provided in Table 1.

4.3. Wastewater tracer and indicator distributions

4.3.1. Chemical tracers

In addition to classifying endmember chemistries, we also characterized the Fishpot Creek sites during monthly samplings to assess the spatial patterns of optical brightener fluorescence values compared to the concentrations of the traditional wastewater tracers B and F^-. The west branch typically had the highest and most variable average optical brightener fluorescence readings (Fig. 2a, b), B concentrations (Fig. 2c, d), and F^- concentrations (Fig. 2e, f), with the most elevated tracer values occurring in the subbasin's headwaters. The outlet had the lowest average optical brightener fluorescence and F^- levels, but featured B concentrations that were elevated relative to the east branch (Fig. 2a–f). Site-specific monthly averages and standard deviations for additional geochemical data are in Table 1, and Pearson's correlations for various parameters are in Table S1. We note that temperature, turbidity, and organic matter content are known to impact fluorescence measurements of optical brighteners. Data for these parameters are given in Tables 1 and 2, and we compare their variations across the catchment in Supplemental Material Section 3.1.

4.3.2. Bacterial indicators and tracers

We analyzed bacteria in Fishpot Creek water samples only during the recreational season (April 1 to October 31 for a given year; Missouri Department of Natural Resources MoDNR, 2016a). While our bacterial sample suite includes one partial recreational season (June 2019 to October 2019) and one full recreational season (April 2020 to October 2020), we describe only the 2020 dataset here because it represents a full recreational season and the data patterns in space and time are similar to those of the 2019 partial recreational season (see Supplemental Material Section 3.2 for information about the entire *E. coli* dataset). While only a small reach in the outlet of the watershed is classified for use (WBC-B), *E. coli* concentrations across the basin commonly exceeded the regulatory value of 206 CFU/100 mL, particularly in the basin headwaters (Fig. 2g, h). Like most of the chemical tracer distributions, we found that the west branch featured the highest geometric mean *E. coli* concentrations, followed by the east branch, then the outlet (Fig. 2g, h).

Since fecal indicator bacteria can originate from multiple sources, we used MST to identify bacterial contamination specifically from humans (i.e., wastewater; see Table 2). General *Bacteroides* was detected in all Fishpot Creek water samples (using the GenBac marker), but human-sourced *Bacteroides* was only detected in three samples (using the HF183 marker). For those three sites, human-associated *Bacteroides* ranged from 0.85 % to 5.07 % of the total *Bacteroides* detected. However, the HF183 concentrations were below the lower limit of quantification, meaning that their concentrations were below the lowest calibration standard.

4.4. Temporal fluctuations in the monitored analytes

Data from high-resolution temporal monitoring at Site 2 (Table 1; Fig. 3) were used to assess the potential variability of our tracers over time. The Site 2 weekly samples had average optical brightener fluorescence, B, and F^- values that were indistinguishable from the monthly data collected at the site (Table 1). Other analyte averages and standard deviations were also consistent between the weekly and monthly sample sets collected at Site 2 (Table 1).

Following flood events (Fig. 3a), optical brightener fluorescence readings tended to increase (Fig. 3b). While we did not find a significant correlation between optical brightener fluorescence measurements and discharge ($r = 0.23, p > 0.05$), we did detect a positive and significant correlation with stage ($r = 0.63, p < 0.05$; Table S2). We did not observe any seasonally driven patterns in our optical brightener fluorescence readings, despite higher temperatures (Fig. 3c) and ultraviolet radiation in the summer months that could respectively interfere with optical brightener measurements or enhance optical brightener photodecay. Turbidity (Fig. 3d) and fDOM (Fig. 3e) tended to peak during discharge events, potentially leading to interferences with optical brightener fluorescence readings. The optical brightener fluorescence measurements at Site 2 did not correlate significantly with turbidity ($r = 0.12, p > 0.05$), but did positively and significantly correlate with fDOM values ($r = 0.78, p < 0.05$; Table S2). However, we did not collect our monthly samples during high flow events when turbidity and fDOM levels were highest.

4.5. Optical brightener fluorescence measurement variability and photodecay tests

We tested the consistency of optical brightener fluorescence measurements over time and accounted for potential organic matter detection by measuring both fluorescence reading variability over short periods in the field as well as photodecay behavior in the laboratory. Field optical brightener fluorescence values did not change more than an average of 5 % on short timescales (i.e., over 15–20 min) at the Fishpot Creek sites during baseflow conditions. We used the laboratory photodecay tests from Cao et al. (2009) and Dubber and Gill (2017) in an attempt to corroborate if samples were positive for optical brighteners. However, these photodecay methods had a detection limit of 5 μL/L for optical brighteners (equivalent to 17.2 RFU on our field instrument). Most of the watershed samples (i.e., 80 % of the monthly samples and 95 % of the weekly samples) were below this threshold. Thus, we found that these tests were not applicable to our study site. Additional details for the photodecay laboratory experiments are outlined in Supplemental Material Section 3.3 and Table S3.

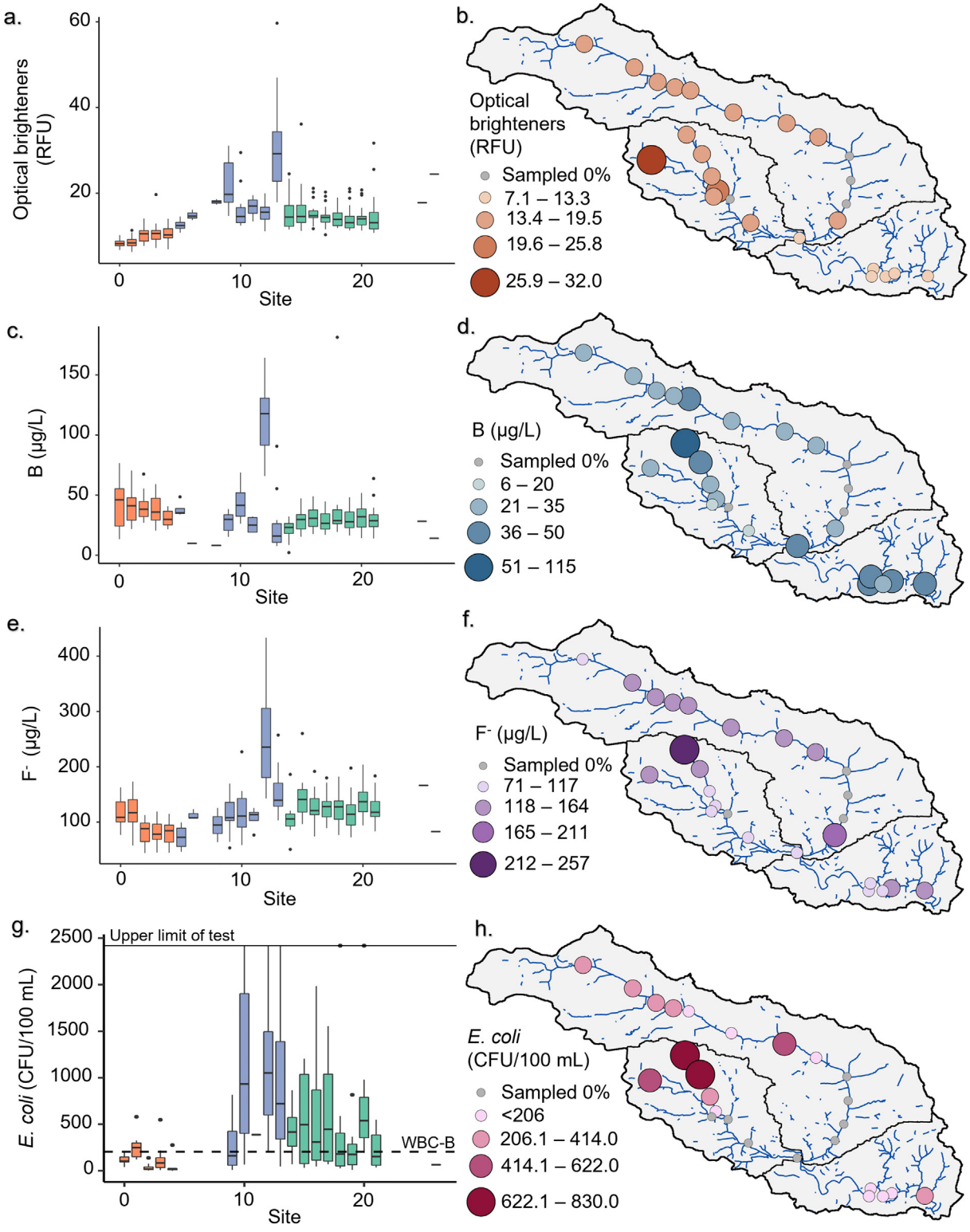

Fig. 2. Optical brightener field fluorescence value (a) median and range for each site (colored by branch; see Fig. 1 for the stream segment color scheme and site locations) and (b) spatial distribution of averages for each site. The optical brightener fluorescence data are for the entire sampling period. The same style plots are shown for B (c and d) and F^- (e and f) concentrations for the whole sampling period. The 2020 recreational season (i.e., April 1, 2020 through October 31, 2020) *E. coli* concentration (g) median and range and (h) geometric mean for each site are also shown. Lines in g indicate the upper limit of the test at 2419.6 CFU/100 mL (solid line) and the regulatory WBC-B limit at 206 CFU/100 mL (dashed line). In the watershed map scales, parameters range from the lowest to the highest average observed value on a linear scale, with the exception of the *E. coli* results, which start at the WBC-B limit of 206 CFU/100 mL and range to the highest average value observed.

Table 2
The MST, *E. coli*, field optical brightener fluorescence, and TOC measurements for the October 26, 2020 watershed samples and method blank.

Sample	GenBac (copies of 16S rRNA/100 mL)	HF183 (copies of 16S rRNA/100 mL)	HF183 (%)	*E. coli* (CFU/100 mL)	Optical brighteners (RFU)	TOC (mg/L)
Site 0 (Pettys Spring)	NA	NA	NA	65.1	9.0	16.9
Site 1	4.70×10^5	ND	ND	122.2	11.3	19.9
Site 2	2.00×10^5	ND	ND	77.6	11.3	12.7
Site 3	5.16×10^5	ND	ND	98.4	11.4	13.3
Site 4	NA	NA	NA	26.5	14.0	13.9
Site 9	7.79×10^5	ND	ND	272.3	30.7	28.2
Site 10	5.26×10^5	2.67×10^4	5.07%	1046.2	22.8	24.9
Site 12	1.33×10^6	ND	ND	1119.9	15.5	21.9
Site 13	9.71×10^5	ND	ND	980.4	33.1	17.4
Site 14	6.08×10^5	ND	ND	517.2	19.3	13.8
Site 15	3.52×10^5	ND	ND	307.6	19.8	14.0
Site 16	2.43×10^6	2.06×10^4	0.85%	1986.3	21.1	17.2
Site 17	5.62×10^5	ND	ND	1553.1	19.3	20.4
Site 18	5.22×10^5	ND	ND	>2419.6	19.0	19.1
Site 19	1.95×10^5	ND	ND	365.4	18.8	18.1
Site 20	5.19×10^5	2.06×10^4	3.98%	2419.6	19.9	18.7
Site 21	1.09×10^5	ND	ND	435.2	19.1	17.9
Method Blank	ND	ND	ND	<1.0	NA	NA

ND = not detected.
NA = not applicable.

4.6. Wastewater contributions to the watershed determined with endmember mixing models

Three mixing models were used to evaluate the fraction of untreated wastewater entering the Fishpot Creek watershed (Fig. 4). Given that the basin does not feature any treated effluent discharge sites or combined sewer overflows, the only potential origin of sanitary sewage is non-point source exfiltration from wastewater infrastructure or septic systems. The two component mixing model utilized optical brightener fluorescence measurements as the wastewater tracer to calculate the contributions of natural water and untreated wastewater to the basin. This approach was tested as a simple endmember separation method for water managers to quickly assess untreated wastewater inputs to a site using only optical brightener fluorescence data. The three component and inverse mixing models included additional tracers to assess natural water and untreated wastewater contributions to the catchment as well as a third potential endmember input to the stream of significance to water managers: drinking water derived from infrastructure leaks or lawn irrigation.

4.6.1. Variations in wastewater inputs across the watershed

The two component mixing model, using only optical brightener fluorescence measurements as the wastewater tracer, predicted that untreated wastewater contributions to the watershed for all monthly samples was, on average, 7 % of the flow, with a standard deviation of ±4 %. Calculated wastewater inputs were highest and most variable among sites in the west branch, particularly at Sites 9 and 13 (Fig. 4a). The lowest and least variable wastewater input predictions for the watershed were observed at the outlet.

For the three component mixing model, we tested three combinations of tracers (optical brighteners and B, optical brighteners and F^-, and B and F^-) that had markedly different concentrations among our endmembers (Fig. 5). We found the best model output resulted from using optical brightener and F^- data (Fig. 4b), meaning we were most frequently able to converge on an answer for the model. Specifically, when running 10,000 iterations of the three component mixing model, the model converged on an answer 32 % of the time using optical brighteners and F^- as the tracers for the monthly samples, with the other combinations converging 12 % (optical brighteners and B) and 10 % (B and F^-) of the time. The average basin-wide untreated wastewater input predicted using monthly optical brightener and F^- data for the three component mixing model was 3 ± 2 % of flow (Fig. 4b), with 92 ± 2 % natural water and 5 ± 2 % drinking water inputs. While calculated untreated wastewater contributions were systematically lower and less variable using the three component mixing model compared to the two component mixing model, the spatial patterns across the basin were similar.

The inverse mixing model (using optical brighteners, B, F^-, Ca, Mg, Sr, and K as tracers) successfully converged on a result 45 % of the time for the monthly spatial samples, returning a solution more frequently than the three component mixing model. The inverse mixing model indicated an average untreated wastewater input to flow of 5 ± 3 % (Fig. 4c), with 67 ± 6 % natural water and 28 ± 7 % drinking water contributions across the basin. While the average untreated wastewater input calculated with the inverse mixing model was only slightly higher than the three component mixing model, the inverse mixing model suggested a much larger drinking water contribution to the watershed. The spatial patterns of untreated wastewater inputs among sites predicted by the inverse mixing model were similar to the two and three component mixing model results.

4.6.2. Variations in wastewater inputs over time

The same three mixing models were used to assess untreated wastewater inputs at high temporal resolution for Site 2. While the calculated untreated wastewater contributions were similar among all the models, ranging 1–4 % of the total flow on average, the inverse mixing model indicated higher drinking water contributions for the site than the three component mixing model. These observations of the relative proportions of each endmember fraction were consistent with model outputs for our spatial data. Overall, our higher resolution temporal data showed relatively little change in untreated wastewater inputs to stream baseflow over time. Additional results for the endmember fractions at the weekly sampling site are outlined in Supplemental Material Section 3.4.

5. Discussion

5.1. Comparison of optical brightener fluorescence readings with traditional wastewater tracer and indicator measurements

We assessed the relationships between optical brighteners and traditional tracers and indicators of wastewater for our samples to determine the utility of using optical brightener fluorescence measurements as an in situ tool for rapid wastewater detection. We expected that as untreated wastewater inputs increased in a given portion of the watershed, so would the optical brightener fluorescence values detected by our handheld field instrument. Likewise, if other analytes were sufficient tracers of wastewater, their concentrations would also increase with more sanitary sewage contributions to the catchment.

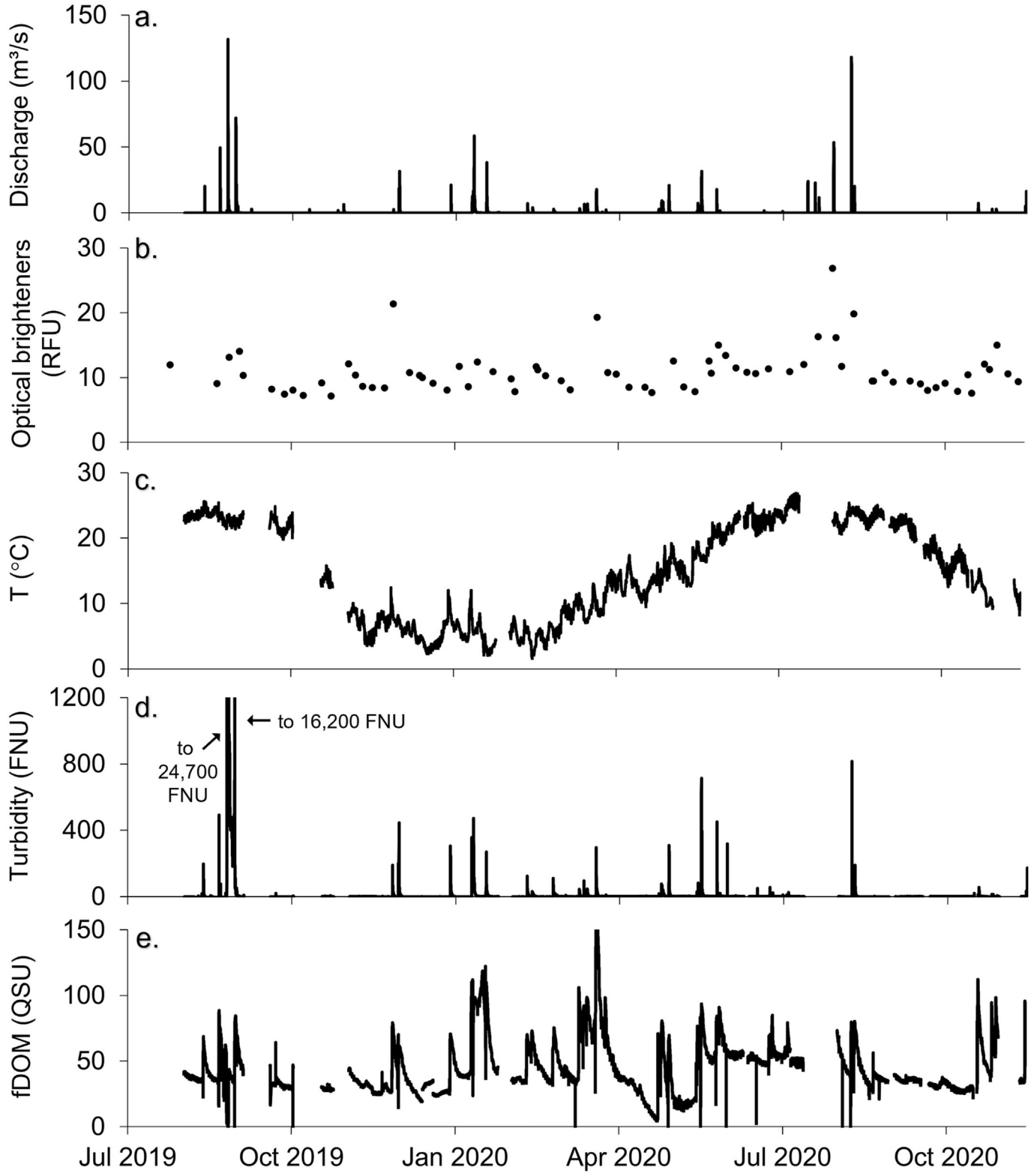

Fig. 3. Data collected from the temporal monitoring site (Site 2; see Fig. 1 for the site location). (a) Discharge data are from USGS gauge 07019120 (USGS, 2022), while (b) optical brightener field fluorescence values are from weekly site visits. Continuous measurements of (c) temperature in °C, (d) turbidity in Formazin Nephelometric Units (FNU), and (e) fDOM in quinine sulfate units (QSU) are also provided as these parameters have been reported to influence optical brightener fluorescence measurements.

5.1.1. Chemical tracers

When all samples were considered, optical brightener fluorescence values and B were not correlated ($r = -0.06$ and $p > 0.05$ for the monthly samples in Table S1 and $r = -0.01$ and $p > 0.05$ for the weekly samples in Table S2). We note that the B concentrations in our Fishpot Creek samples were often lower than those observed for the natural endmember, Rockwoods Spring (Fig. 5a, c). Lower B concentrations in the Fishpot Creek samples than the selected natural endmember may be the result of differences in natural water composition

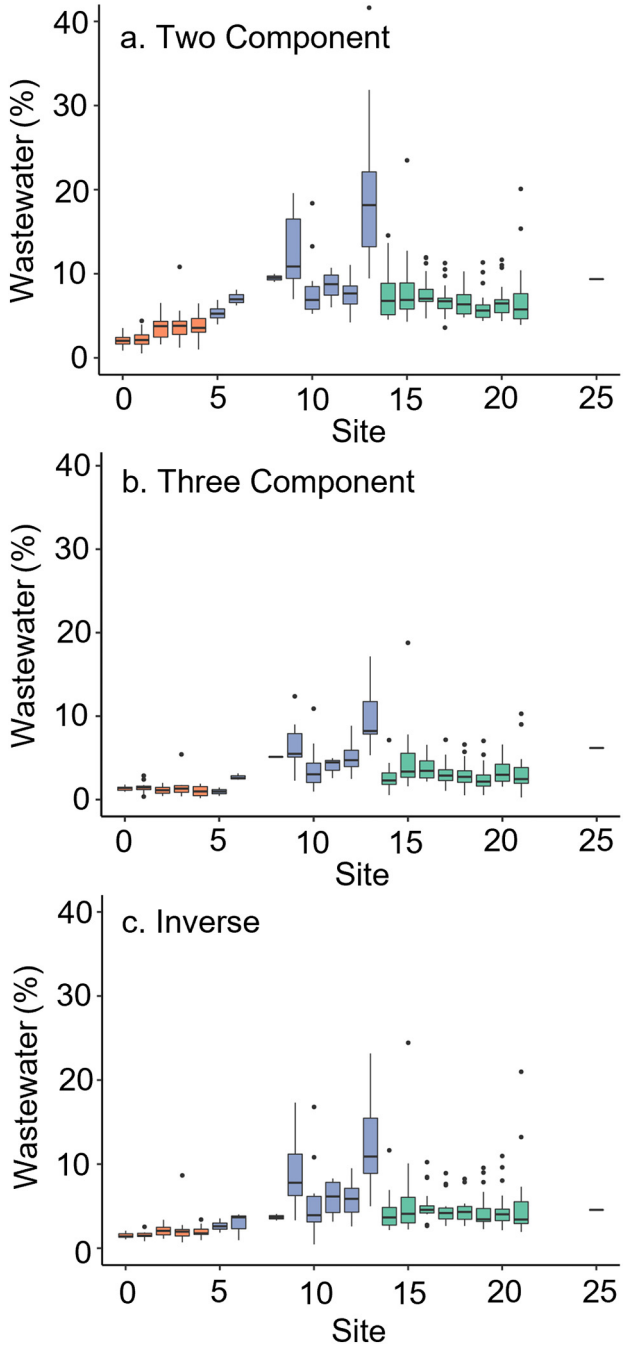

Fig. 4. The (a) two component (tracer: optical brightener fluorescence values), (b) three component (tracers: optical brightener fluorescence and F^- values), and (c) inverse (tracers: optical brightener fluorescence, B, F^-, Ca, Mg, Sr, and K values) mixing model results for the percent untreated wastewater in the Fishpot Creek watershed monthly samples by site. See Fig. 1 for the stream segment color scheme and site locations.

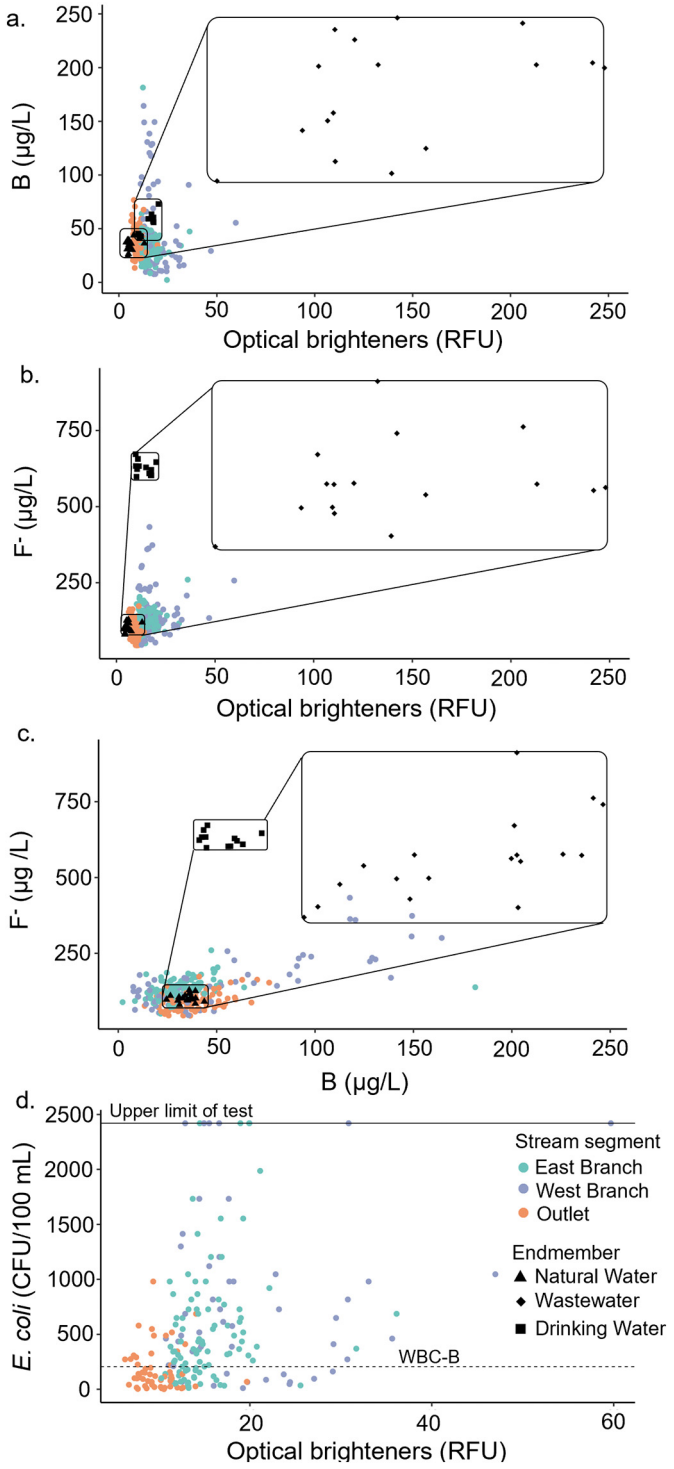

Fig. 5. Mixing diagrams for (a) optical brightener fluorescence measurements and B concentrations, (b) optical brightener fluorescence measurements and F^- concentrations, and (c) B and F^- concentrations for the monthly Fishpot Creek watershed samples. Boxes indicate the analyte value ranges for the three endmembers: natural water (triangles), untreated wastewater (diamonds), and drinking water (squares). A plot of (d) optical brightener fluorescence values and *E. coli* concentrations is also provided, but we note that *E. coli* data were only collected during the recreational season and endmember *E. coli* values are not available.

across the study region. These observations indicate that B cannot be universally used on its own to identify wastewater contributions to watersheds as B inputs may come from sources other than bleaching agents in detergents (e.g., rock weathering or fertilizers; Hasenmueller and Criss, 2013). For example, we observed relatively elevated B levels near the spring-fed outlet of the watershed (Fig. 2c, d), where optical brightener fluorescence signals were the lowest (Fig. 2a, b). A longer residence time for the groundwater that enters the stream could increase B concentrations through water-rock interactions thereby convoluting the sanitary sewage-related B signature and decreasing the efficacy of B as a wastewater tracer.

Most of the watershed samples fell within the bounds of the endmember mixing diagram for optical brightener fluorescence and F^- data (Fig. 5b). Nevertheless, some of our stream samples had lower F^- concentrations

than the natural water endmember, again indicating that the natural endmember used for the study may not be ideal. Watershed optical brightener fluorescence values and F^- concentrations had a significant ($p < 0.05$) but weak positive correlation ($r = 0.18$ for the monthly samples in Table S1 and $r = 0.34$ for the weekly samples in Table S2). This weak relationship is likely due to contributions of F^- to the catchment from sources other than wastewater. Indeed, we observed two clusters of data in our mixing diagram, predominantly comprised of samples from the west branch (Fig. 5b). In both groupings, F^- concentrations correlated with optical brightener fluorescence measurements, but the regressions trended towards either the wastewater endmember or the drinking water endmember. These data trends suggest that some reaches of the stream may be more impacted by wastewater inputs, while other areas of the basin may receive higher drinking water contributions. Because F^- can be sourced from both wastewater and drinking water, it consequently cannot be used by itself to determine wastewater inputs to the environment.

5.1.2. Bacterial indicators and tracers

Fecal indicator bacteria, like *E. coli*, are commonly used to help detect wastewater infrastructure issues. While *E. coli* measurements are an inexpensive and straightforward test to understand fecal contamination of water resources, they cannot be used to distinguish human-sourced bacteria from other origins. We observed a positive ($r = 0.30$) and significant ($p < 0.05$) correlation between optical brightener fluorescence levels and *E. coli* concentrations, but the correlation r value was low and the data scatter was high (Fig. 5d; Table S1), indicating *E. coli* sources to the catchment other than untreated wastewater. Evidence for non-human origins of *E. coli* to the watershed was demonstrated by our MST results (Table 2). While the sites that were positive for human-associated *Bacteroides* also had relatively high *E. coli* concentrations of ≥1046.2 CFU/100 mL, 75 % of the sites that were above the WBC-B limit of 206 CFU/100 mL and 50 % of the sites with *E. coli* concentrations ≥1046.2 CFU/100 mL contained no human-associated *Bacteroides*. Thus, most of the sites with elevated *E. coli* levels had bacterial contamination from non-human sources (e.g., pet or wildlife waste). This result illustrates that use of fecal indicator bacteria alone could confound water manager's efforts to identify faulty wastewater infrastructure.

When comparing optical brightener fluorescence values with the MST results for the October 2020 samples (Table 2), we found that the highest optical brightener sensor response values (>30.0 RFU at Sites 9 and 13) did not correspond with samples that were positive for human fecal inputs. Both Sites 9 and 13 featured large stormwater sewer lines that drained to the stream sampling locations, implying that the observed optical brightener signatures may have had other sources besides sanitary sewage (e.g., detergents used to wash vehicles that subsequently entered the stormwater sewer system). While Site 9 featured a high TOC concentration of 28.2 mg/L, which could potentially interfere with field optical brightener fluorescence readings, Site 13's TOC value of 17.4 mg/L was below the average for all sites (Table 2), indicating organic matter interferences may not be the cause of high optical brightener fluorescence readings at these sites. The next three highest optical brightener fluorescence measurements (19.9–22.8 RFU at Sites 10, 16, and 20) correspond with the three basin locations that were positive for HF183, the human-associated *Bacteroides*. These sites did not feature prominent stormwater inputs, indicating that optical brightener fluorescence signals and human-derived bacteria at these locations are likely sourced from sanitary sewage. We observed that all sites with optical brightener fluorescence values ≤19.8 RFU tested negative for human-associated *Bacteroides*, suggesting a potential threshold optical brightener fluorescence signal for indicating the presence of untreated sanitary sewage in the watershed.

5.2. Wastewater tracer and indicator relationships with infrastructure distribution

We compared wastewater tracers and indicators with infrastructure density through the basin because areas of high sewer pipe density likely represent reaches of the stream that are more prone to receive inputs of sanitary sewage from leaks in the system. Of the wastewater tracers and indicators we used (i.e., optical brighteners, B, F^-, *E. coli*), we found that optical brightener fluorescence values had the strongest correlation with sewer infrastructure density ($r = 0.71, p < 0.05$; Table S1). Other chemical tracers, like B and F^-, had no to weak, non-significant correlations with wastewater infrastructure density ($r \leq 0.25, p > 0.05$; Table S1), suggesting other sources for these analytes such as rock weathering, fertilizer, or treated drinking water inputs. While *E. coli* levels had a significant ($p < 0.05$) and positive correlation with wastewater infrastructure density, the correlation was weak ($r = 0.29$; Table S1) due to multiple sources of *E. coli* in the watershed (e.g., pet or wildlife waste). Our findings imply that optical brightener fluorescence measurements may not only be a rapid, in situ test for untreated wastewater, but they are likely more effective tracers in catchments where traditional wastewater tracer and indicator signatures are confounded by other sources.

5.3. Characterization of wastewater inputs to the watershed using endmember mixing models

Using our two component, three component, and inverse mixing models for the monthly spatial data, we found significant, positive correlations between the average percentage of wastewater to flow and sewer pipe density at each subcatchment (Fig. 6). These results indicate that areas of the basin with higher wastewater infrastructure densities have higher wastewater inputs. While the calculated wastewater contributions for the sites were similar among the models, the two component mixing model generally yielded slightly higher wastewater fractions. This model also produced the strongest correlation between the wastewater fraction and sewer infrastructure density ($r = 0.86$, $p < 0.05$; Fig. 6), suggesting the simpler model may be ideal for wastewater detection studies conducted by water managers.

For both the three endmember and inverse mixing models, we observed model success rates of <50 %, with some tracer combinations in the three endmember mixing model converging on a result only 10 % of the time. The higher success rate of 32 % for iterations of the three component mixing model using optical brightener fluorescence measurements and F^- concentrations (compared to other tracer combinations) was likely because a majority of the watershed chemical data fell within the three endmember concentration ranges for these analytes (Fig. 5b). In cases where the models failed to converge on apportioned endmember results, narrow ranges for some endmember chemistries and/or endmembers for which we did not account (e.g., potential B inputs from rock weathering or fertilizers) may be the cause. Indeed, B concentrations in our natural endmember were often higher than those in our stream samples (Fig. 5a, c). Nevertheless, we note that the chemical composition of wastewater was highly variable for all analytes, including optical brightener fluorescence values (Table 1; Fig. 5), making wastewater tracer studies inherently challenging.

5.4. Utility of in situ optical brightener fluorescence measurements for wastewater assessments

Optical brightener fluorescence is a fast, easy, and inexpensive measurement that can be used as an initial way to screen waterbodies in the field for wastewater contributions. Their readings are also the only option for in situ wastewater testing. Not only do optical brightener fluorescence values have the strongest positive correlation with wastewater infrastructure density of any parameter we measured (Table S1), but other tracers and indicators (e.g., B, F^-, *E. coli*) had contributions to the watershed from sources other than wastewater (e.g., rock weathering, fertilizers, drinking water, pet and wildlife waste) that caused their weaker correlations with wastewater infrastructure density. Our data indicate that optical brighteners are ideal tracers for detecting potential untreated wastewater inputs to the environment, likely because they have few (and no natural) sources to confound in situ readings.

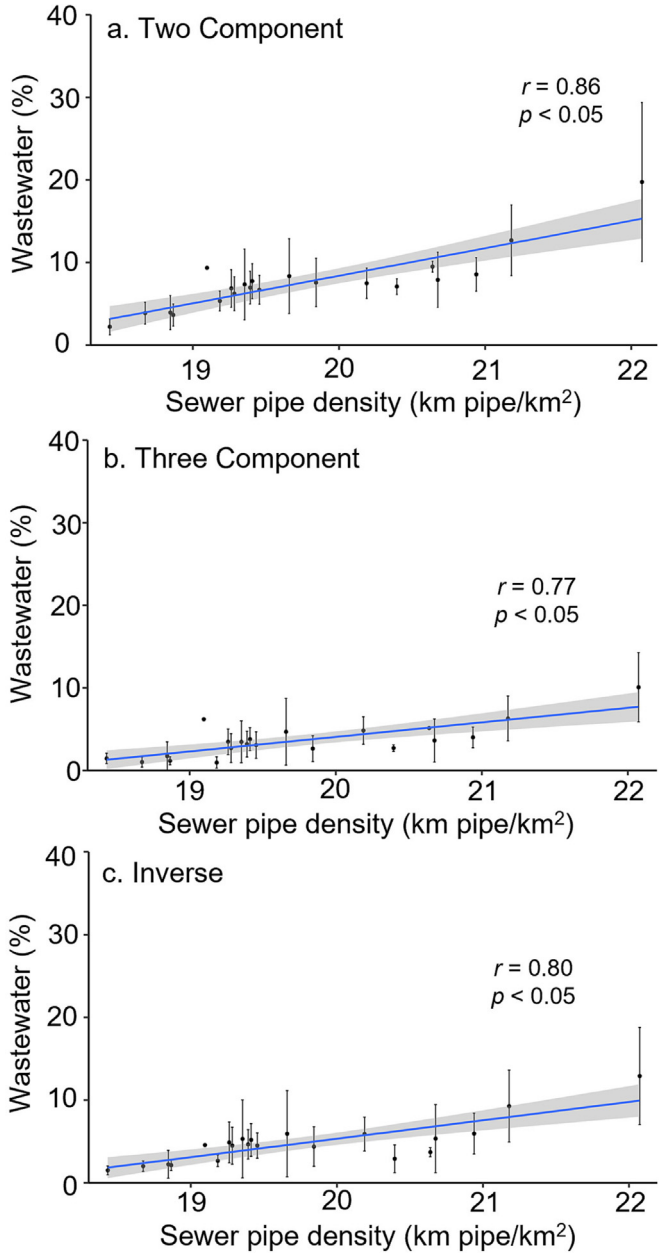

Fig. 6. Average untreated wastewater percentage of flow calculated from the (a) two component, (b) three component, and (c) inverse mixing models as a function of sewer pipe density in each sampling site's subcatchment. Bars indicate the standard deviation of the wastewater endmember fraction at each site across the sampling period.

5.5. Limitations of in situ optical brightener fluorescence measurements for wastewater assessments

Prior studies have observed that intense ultraviolet light, especially in the summer, can degrade optical brighteners in water (Cao et al., 2009; Dubber and Gill, 2017), both when samples were exposed to strong sunlight or kept in the shade (Cao et al., 2009). However, we did not detect any seasonal oscillations in optical brightener fluorescence measurements at our temporal monitoring location (Site 2; Fig. 3). We suspect that either heavy shading from the riparian zone or the short residence time of the water in the stream may have reduced the potential for optical brightener photodecay at our study site. Nevertheless, photodecay of optical brighteners may be an issue for other systems.

Organic matter interferences have also been suggested as a potential limitation for in situ optical brightener assessments (Hartel et al., 2007; Dubber and Gill, 2017). We indeed observed a positive and significant correlation between optical brightener fluorescence and fDOM measurements at Site 2 ($r = 0.78, p < 0.05$; Table S2), suggesting the potential detection of dissolved organic matter with our handheld fluorometer. We note, however, that optical brightener fluorescence readings, fDOM, and stage were all significantly and positively correlated with each other at the temporal monitoring site (Table S2). These intercorrelations indicate that organic matter interferences with the optical brightener fluorescence readings were likely minimized during baseflow conditions (like when we sampled across the watershed) because organic matter content in the water was low. When we attempted to use photodecay patterns to assess these potential interferences in watershed samples (see Supplemental Material Section 3.3 for more detail), we found that most of our samples were below the method detection limit of 5 μL/L (17.2 RFU on our handheld field instrument). Our findings indicate these photodecay tests may not be appropriate for samples with low optical brightener concentrations.

6. Conclusion

We showed that in situ optical brightener fluorescence readings can be used as a rapid reconnaissance tool to identify wastewater inputs in watersheds. Their measurements were more robust for wastewater detection than traditional tracers and indicators (e.g., B, F^-, *E. coli*), which often have sources other than sanitary sewage. Indeed, our data showed that, of all the tracers we measured, optical brightener fluorescence values had the best correlation with wastewater infrastructure density, were elevated when human-associated fecal bacteria were present in our watershed samples, and produced the best mixing model outputs, indicating their utility as wastewater tracers. We therefore recommend the use of in situ measurements of optical brightener fluorescence as an initial screening tool for sanitary sewage inputs to the environment.

Users need to be aware of some limitations for this method, however, including artificially low readings due to photodecay by ultraviolet light or erroneously high readings due to interferences with organic matter. These challenges can be reduced if sample collection occurs on days when both ultraviolet light exposure and flow conditions are low. Water samples that have high in situ optical brightener fluorescence values should be validated for the presence of wastewater with other tools, such as MST and chemical analyses, to further investigate the potential for wastewater contributions to the site of interest. Nevertheless, optical brighteners are ideal tracers for reconnaissance studies to identify potential problems with wastewater infrastructure because they are quickly, easily, and inexpensively measured with handheld fluorometers in the field. Our rapid detection technique can be used to guide further sampling and wastewater infrastructure remediation efforts.

Supplementary data to this article can be found online at https://doi.org/10.1016/j.scitotenv.2023.163378.

CRediT authorship contribution statement

Carly R. Finegan: Conceptualization, Data curation, Formal analysis, Funding acquisition, Investigation, Methodology, Visualization, Validation, Writing - original draft preparation.

Elizabeth A. Hasenmueller: Conceptualization, Formal analysis, Funding acquisition, Methodology, Resources, Writing - review and editing, Supervision.

Data availability

Data will be made available on request.

Declaration of competing interest

The authors declare that they have no known competing financial interests or personal relationships that could have appeared to influence the work reported in this paper.

Acknowledgements

This work was funded by research grants from the Metropolitan Saint Louis Sewer District (MSD) to EAH and the Geological Society of America (GSA) Graduate Student Research Grant (12847-20) program to CRF as well as other funds from Saint Louis University. Elemental data for this study were collected on a Perkin Elmer Optima 8300 ICP-OES funded by the National Science Foundation (CHE-1626501) and Saint Louis University. We thank Jay Hoskins, Kirk Lambrecht, and Jim Hessel at MSD for providing logistical support, sewer infrastructure data, and monthly wastewater samples as well as many field and laboratory assistants for their help with the project. We appreciate the comments from two anonymous reviewers, which helped us improve the manuscript.

References

Anderson, K.L., Whitlock, J.E., Harwood, V.J., 2005. Persistence and differential survival of fecal indicator bacteria in subtropical waters and sediments. Appl. Environ. Microbiol. 75 (6), 3041–3048. https://doi.org/10.1128/AEM.71.6.3041-3048.2005.

Bird, K., Boopathy, R., Nathaniel, R., LaFleur, G., 2019. Water pollution and observation of acquired antibiotic resistance in Bayou Lafourche, a major drinking water source in Southeast Louisiana, USA. Environ. Sci. Pollut. Res. 26 (33), 34220–34232. https://doi.org/10.1007/s11356-018-4008-5.

Cao, Y., Griffith, J.F., Weisberg, S.B., 2009. Evaluation of optical brightener photodecay characteristics for detection of human fecal contamination. Water Res. 43 (8), 2273–2279. https://doi.org/10.1016/j.watres.2009.02.020.

Criss, R.E., Davisson, M.L., Kopp, J.W., 2001. Nonpoint sources in the lower Missouri River. J. Am. Water Works Assoc. 93, 112–122. https://doi.org/10.1002/j.1551-8833.2001.tb09131.x.

Dickenson, E., Snyder, S., Sedlak, D., Drewes, J., 2011. Indicator compounds for assessment of wastewater effluent contributions to flow and water quality. Water Res. 45, 1199–1212. https://doi.org/10.1016/j.watres.2010.11.012.

Dickerson, J.W., Hagedorn, C., Hassall, A., 2007. Detection and remediation of human-origin pollution at two public beaches in Virginia using multiple source tracking methods. Water Res. 41 (16), 3758–3770. https://doi.org/10.1016/j.watres.2007.02.055.

Devane, M.L., Moriarty, E.M., Robson, B., Lin, S., Wood, D., Webster-Brown, J., Gilpin, B.J., 2019. Relationships between chemical and microbial faecal source tracking markers inurban riverwater and sediments during and post-discharge of human sewage. Sci. Total Environ. 651, 1588–1604. https://doi.org/10.1016/j.scitotenv.2018.09.258.

Dubber, D., Gill, L.W., 2017. Suitability of fluorescent whitening compounds (FWCs) as indicators of human faecal contamination from septic tanks in rural catchments. Water Res. 127, 104–117. https://doi.org/10.1016/j.watres.2017.10.005.

Guinoiseau, D., Louvat, P., Paris, G., Chen, J.B., Chetelat, B., Rocher, V., Guérin, S., Gaillardet, J., 2018. Are boron isotopes a reliable tracer of anthropogenic inputs to rivers over time? Sci. Total Environ. 626, 1057–1068. https://doi.org/10.1016/j.scitotenv.2018.01.159.

Hagedorn, C., Saluta, M., Hassall, A., Dickerson, J., 2005. Fluorometric detection of optical brighteners as an indicator of human sources of water pollution. Part I: Description and detection of optical brighteners. Crop and Soil Environmental News. Online periodical accessed at https://www.sites.ext.vt.edu/newsletter-archive/cses/2005-11/part1.html.

Hagedorn, C., Saluta, M., Hassall, A., Dickerson, J., 2005. Fluorometric detection of optical brighteners as an indicator of human sources of water pollution. Part II: Development as a source tracking methodology. Crop and Soil Environmental News. Online periodical accessed at https://www.sites.ext.vt.edu/newsletter-archive/cses/2005-11/part2.html.

Hartel, P.G., Hagedorn, C., McDonald, J.L., Fisher, J.A., Saluta, M.A., Dickerson, J.W., Gentit, L.C., Smith, S.L., Mantripragada, N.S., Ritter, K.J., Belcher, C.N., 2007. Exposing water samples to ultraviolet light improves fluorometry for detecting human fecal contamination. Water Res. 41 (16), 3629–3642. https://doi.org/10.1016/j.watres.2007.03.034.

Hasenmueller, E.A., Criss, R.E., 2013. Multiple sources of boron in urban surface waters and groundwaters. Sci. Total Environ. 447, 235–247. https://doi.org/10.1016/j.scitotenv.2013.01.001.

Homer, C.G., Dewitz, J.A., Yang, L., Jin, S., Danielson, P., Xian, G., Coulston, J., Herold, N.D., Wickham, J.D., Megown, K., 2015. Completion of the 2011 National Land Cover Database for the conterminous United States – representing a decade of land cover change information. Photogramm. Eng. Remote Sensing 81 (5), 345–354. https://doi.org/10.1016/S0099-1112(15)30100-2.

IDEXX Laboratories, 2013. Quanti-Tray/2000 Insert and Most Probable Number (MPN) Table.

IDEXX Laboratories, 2017. Colilert -18 procedure. Water Analysis Methods.

Kennedy, M.S., Sarikelle, S., Suravallop, K., 1991. Calibrating hydraulic analyses of distribution-systems using fluoride tracer studies. J. Am. Water Works Assoc. 83 (7), 54–59. https://doi.org/10.1002/j.1551-8833.1991.tb07179.x.

Lee, E.S., Krothe, N.C., 2001. A four-component mixing model for water in a karst terrain in south-Central Indiana, USA. Using solute concentration and stable isotopes as tracers. Chem. Geol. 179, 129–143. https://doi.org/10.1016/S0009-2541(01)00319-9.

Lockmiller, K.A., Wang, K., Fike, D.A., Shaughnessy, A.R., Hasenmueller, E.A., 2019. Using multiple tracers (F^-, B, $\delta^{11}B$, and optical brighteners) to distinguish between municipal drinking water and wastewater inputs to urban streams. Sci. Total Environ. 671, 1245–1256. https://doi.org/10.1016/j.scitotenv.2019.03.352.

Meenakshi, Maheshwari, R.C., 2006. Fluoride in drinking water and its removal. Journal of Hazardous Materials 137 (1), 456–463. https://doi.org/10.1016/J.JHAZMAT.2006.02.024.

Metropolitain Saint Louis Sewer District, 2019. Sanitary and Stormwater Sewer Infrastructure GIS Data for the St. Louis, Missouri Area. MSD Obtained 2019.

Missouri American Water, 2019. 2019 Annual water quality report: St. Louis County and St. Charles County (Issue 866). Retrieved from https://www.amwater.com/ccr/champaign.pdf.

Missouri Department of Natural Resources (MoDNR), 2016a. Total Maximum Daily Load (TMDL) for Fishpot Creek, St. Louis County, Missouri.

Missouri Department of Natural Resources (MoDNR), 2016b. 2016 environmental protection agency approved 303(d) listed waters. Missouri Department of Natural Resources, Water Protection Program. Retrieved from https://dnr.mo.gov/document/2016-epa-approved-section-303d-listed-waters.

Négrel, P., Allègre, C.J., Dupré, B., Lewin, E., 1993. Erosion sources determined by inversion of major and trace element ratios and strontium isotopic ratios in river water: the Congo Basin case. Earth Planet. Sci. Lett. 120 (1–2), 59–76. https://doi.org/10.1016/0012-821X(93)90023-3.

Petelet-Giraud, E., Klaver, G., Negrel, P., 2009. Natural versus anthropogenic sources in the surface- and groundwater dissolved load of the dommel river (Meuse basin): constraints by boron and strontium isotopes and gadolinium anomaly. J. Hydrol. 369 (3–4), 336–349. https://doi.org/10.1016/j.jhydrol.2009.02.029.

Poiger, T., Field, J.A., Field, T.M., Siegrist, H., Giger, W., 1998. Behavior of fluorescent whitening agents during sewage treatment. Water Res. 32 (6), 1939–1947. https://doi.org/10.1016/S0043-1354(97)00408-9.

Rabiet, M., Brissaud, F., Seidel, J.L., Pistre, S., Elbaz-Poulichet, F., 2005. Deciphering the presence of wastewater in a medium-sized Mediterranean catchment using a multitracer approach. Appl. Geochem. 20 (8), 1587–1596. https://doi.org/10.1016/j.apgeochem.2005.04.005.

Robinson, H.K., Hasenmueller, E.A., 2017. Transport of road salt contamination in karst aquifers and soils over multiple timescales. Sci. Total Environ. 603–604, 94–108. https://doi.org/10.1016/j.scitotenv.2017.05.244.

Roy, S., Gaillardet, J., Allègre, C.J., 1999. Geochemistry of dissolved and suspended loads of the seine river, France: anthropogenic impact, carbonate and silicate weathering. Geochim. Cosmochim. Acta 63 (9), 1277–1292. https://doi.org/10.1016/S0016-7037(99)00099-X.

Sklash, M.G., Farvolden, R.N., Fritz, P., 1976. A conceptual model of watershed response to rainfall, developed through the use of oxygen-18 as a natural tracer. Can. J. Earth Sci. 13 (5), 715. https://doi.org/10.1139/e76-076.

Tavares, M.E., Spivey, M.I.H., McIver, M.R., Mallin, M.A., 2008. Testing for optical brighteners and fecal bacteria to detect sewage leaks in tidal creeks. J. N. C. Acad. Sci. 124 (3), 91–97 Accessed at https://dc.lib.unc.edu/cgi-bin/showfile.exe?CISOROOT=/jncas&CISOPTR=3904.

United States Department of Health and Human Services Federal Panel on Community Water Fluoridation (USDHHS), 2015. United States Public Health Service Recommendation for Fluoride Concentration in Drinking Water for the Prevention of Dental Caries. Public Health Rep. 130 (4), 318–331. https://doi.org/10.1177/003335491513000408 PMID: 26346489; PMCID: PMC4547570.

United States Environmental Protection Agency (USEPA), 2018. 2017 Five-year review of the 2012 recreational water quality criteria. Office of Water, Office of Science and Technology (Issue May) https://doi.org/10.3748/wjg.v19.i24.3761.

United States Environmental Protection Agency (USEPA), 2019. . (March)Method 1696: Characterization of Human Fecal Pollution in Water by HF183/BacR287 TaqMan ® Quantitative Polymerase Chain Reaction (qPCR) Assay. 821. EPA Office of Water, pp. 2–19.. www.epa.gov.

United States Geological Survey (USGS), 2022. National Water Information System (NWIS) data for USGS 07019120 Fishpot Creek at Valley Park, MO. https://waterdata.usgs.gov/mo/nwis/uv?site_no=07019120.

Van Stempvoort, D.R., Roy, J.W., Grabuski, J., Brown, S.J., Bickerton, G., Sverko, E., 2013. An artificial sweetener and pharmaceutical compounds as co-tracers of urban wastewater in groundwater. Sci. Total Environ. 461–462, 348–3359. https://doi.org/10.1016/j.scitotenv.2013.05.001.

Vengosh, A., Heumann, K.G., Juraske, S., Kasher, R., 1994. Boron isotope application for tracing sources of contamination in groundwater. Environ. Sci. Technol. 28 (11), 1968–1974. https://doi.org/10.1021/es00060a030.